

SCRIPPS INSTITUTION OF OCEANOGRAPHY LA JOLLA CA VISA--ETC P/O 20/6
DAYTIME VISIBILITY, A CONCEPTUAL REVIEW, (U) F19620-70-C-0200
NOV 79 J I GORDON
SIO-REF-80-1 AFSL-TR-79-0257 ML

UNCLASSIFIED

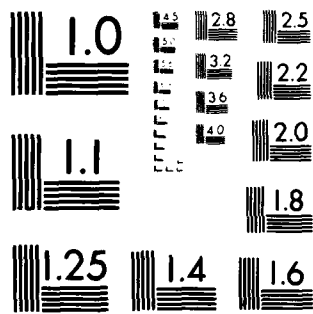
AFGL-TR-79-0257

14

Page 10 of 10

21) $\frac{1}{2} \log_2 2$

END
DATE
FILMED
7-80
DTIC



MICROCOPY RESOLUTION TEST CHART
NATIONAL BUREAU OF STANDARDS-1963-A

LEVEL #

(12) SC

AFGL-TR-79-0257

SIO Ref. 80-1

ADA 085451

DAYTIME VISIBILITY, A Conceptual Review

Jacqueline I. Gordon

Approved for public release; distribution unlimited.

Scientific Report No. 11
November 1979

Contract No. F19628-78-C-0200
Project No. 7670
Task No. 7670-14
Work Unit No. 7670-14-01

Contract Monitor, Major T. S. Cross, USAF
Optical Physics Division

Prepared for
Air Force Geophysics Laboratory, Air Force Systems Command
United States Air Force, Hanscom AFB, Massachusetts 01731

DTIC
ELECTE
JUN 1 6 1980
S D
A

80 6 13 035

1

THE UNIVERSITY OF CHICAGO PRESS
CHICAGO, ILLINOIS 60637
U.S.A.

UNCLASSIFIED

SECURITY CLASSIFICATION OF THIS PAGE (When Data Entered)

REPORT DOCUMENTATION PAGE		READ INSTRUCTIONS BEFORE COMPLETING FORM
1. REPORT NUMBER 18 AFGL TR-79-0257	2. GOVT ACCESSION NO. AD-A085 451	3. RECIPIENT'S CATALOG NUMBER
4. TITLE (and Subtitle) DAYTIME VISIBILITY, A Conceptual Review		5. TYPE OF REPORT & PERIOD COVERED Scientific Report No. 11
7. AUTHOR(s) Jacqueline I. Gordon		6. PERFORMING ORG. REPORT NUMBER SIO Ref. 80-1
9. PERFORMING ORGANIZATION NAME AND ADDRESS University of California, San Diego Visibility Laboratory La Jolla, California 92093		8. CONTRACT OR GRANT NUMBER(s) F19628-78-C-0200
11. CONTROLLING OFFICE NAME AND ADDRESS Air Force Geophysics Laboratory Hanscom AFB, Massachusetts 01731 Contract Monitor: Major Cress/OPA		10. PROGRAM ELEMENT, PROJECT, TASK AREA & WORK UNIT NUMBERS 62101F 7670414-01
14. MONITORING AGENCY NAME & ADDRESS (if different from Controlling Office) SIO REF-80-1 CONTRACT F19628-78-C-0200		12. REPORT DATE November 1979
		13. NUMBER OF PAGES 22
		15. SECURITY CLASS. (of this report) UNCLASSIFIED
		15a. DECLASSIFICATION/DOWNGRADING SCHEDULE
16. DISTRIBUTION STATEMENT (of this Report) Approved for public release; distribution unlimited.		
17. DISTRIBUTION STATEMENT (of the abstract entered in Block 20, if different from Report)		
18. SUPPLEMENTARY NOTES		
19. KEY WORDS (Continue on reverse side if necessary and identify by block number) Atmospheric Attenuation Coefficient Atmospheric Beam Transmittance Visibility ALPHA GAMMA EQUAL TO 3		
20. ABSTRACT (Continue on reverse side if necessary and identify by block number) Daytime visibility is defined as the distance a black object can be seen against the horizon sky. Data on visual thresholds for daylight illumination are examined and the degradation of the contrast by the atmosphere described. The visibility as reported in meteorology correlates well with a contrast threshold of 0.05 and thus the attenuation coefficient and threshold sighting range product is equal to 3 ($\alpha r = 3$). Psychophysical data on visual thresholds for 0.33 second glimpse times when corrected to confident viewing with a 4 degree uncertainty of target posi-		

DD FORM 1 JAN 73 1473

EDITION OF 1 NOV 65 IS OBSOLETE
S/N 0102-014-6601

UNCLASSIFIED

SECURITY CLASSIFICATION OF THIS PAGE (When Data Entered)

367000

JRC

UNCLASSIFIED

SECURITY CLASSIFICATION OF THIS PAGE (When Data Entered)

20. ABSTRACT continued:

tion, predict the visibility distances well and indicate that the meteorological observers are using targets subtending on the average about 7.6 minutes of arc. Visibilities have an uncertainty of approximately ± 20 percent in relation to measured physical parameters of air clarity. The errors in visibility distance inherent in the use of non-black targets and backgrounds other than the horizon sky are delineated. Some of the physical methods of measuring air clarity are described with reference to their use in obtaining a measure of visibility.

UNCLASSIFIED


SECURITY CLASSIFICATION OF THIS PAGE (When Data Entered)

DAYTIME VISIBILITY, A Conceptual Review

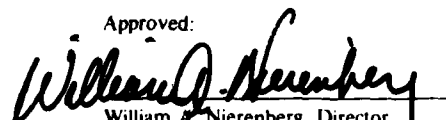
Jacqueline I. Gordon

Visibility Laboratory
University of California, San Diego
Scripps Institution of Oceanography
La Jolla, California 92093

Approved:


Roswell W. Austin, Acting Director
Visibility Laboratory

Approved:


William A. Nierenberg, Director
Scripps Institution of Oceanography

CONTRACT NO. F19628-78-C-0200

Project No. 7670

Task No. 7670-14

Work Unit No. 7670-14-01

Scientific Report No. 11

November 1979

Contract Monitor

Major Ted S. Cress, Atmospheric Optics Branch, Optical Physics Division

Approved for public release; distribution unlimited.

Prepared for

AIR FORCE GEOPHYSICS LABORATORY
AIR FORCE SYSTEMS COMMAND
UNITED STATES AIR FORCE
HANSCOM AFB, MASSACHUSETTS 01731

Accession For	
NTIS G.O.S.I.	<input checked="" type="checkbox"/>
DDC Tag	<input type="checkbox"/>
Unpublished	<input type="checkbox"/>
Justification	<input type="checkbox"/>
By	
Date	
Special	
A	

SUMMARY

Daytime visibility is defined as the distance a black object can be seen against the horizon sky. Data on visual thresholds for daylight illumination are examined and the degradation of the contrast by the atmosphere described. The visibility as reported in meteorology correlates well with a contrast threshold of 0.05 and thus the attenuation coefficient and threshold sighting range product is equal to 3 ($\alpha r=3$). Psychophysical data on visual thresholds for 0.33 second glimpse times when corrected to confident viewing with a 4 degree uncertainty of target position, predict the visibility distances well and indicate that the meteorological observers are using targets subtending on the average about 7.6 minutes of arc. Visibilities have an uncertainty of approximately ± 20 percent in relation to measured physical parameters of air clarity. The errors in visibility distance inherent in the use of non-black targets and backgrounds other than the horizon sky are delineated. Some of the physical methods of measuring air clarity are described with reference to their use in obtaining a measure of visibility.

PRECEDING PAGE BLANK-NOT FILMED

TABLE OF CONTENTS

SUMMARY	v
LIST OF ILLUSTRATIONS	ix
1. INTRODUCTION	1
2. VISUAL THRESHOLDS FOR DAYLIGHT ILLUMINATION	1
3. DEGRADATION OF THE LUMINANCE SIGNAL BY THE ATMOSPHERE	1
4. THRESHOLD CONTRAST OF VISIBILITY TARGETS	2
5. THRESHOLD ANGULAR SIZE OF VISIBILITY TARGETS	5
6. RELATION OF ATTENUATION COEFFICIENT AND THRESHOLD SIGHTING RANGE	7
7. RELATIVE VISUAL RANGE OF NON-BLACK TARGETS	7
Horizon Sky Equivalent Reflectance	8
Horizon Sky Reflectance for Overcast	9
Horizon Sky Reflectance from 4π Radiance Measurements	9
8. BACKGROUNDS OTHER THAN THE CLEAR HORIZON SKY	11
Sky Ground Ratio	12
9. PHYSICAL MEASUREMENT METHODS	13
Luminance Transmittance	13
Attenuation Coefficient	13
Total Volume Scattering Coefficient	13
Diffuse Light Source	14
Cosine Collector	14
Apparent Luminance of Distant Object and Sky	14
10. VISIBILITY BIBLIOGRAPHY	14
11. SUMMARY	14
12. ACKNOWLEDGEMENTS	14
13. REFERENCES	15
APPENDIX	16

LIST OF ILLUSTRATIONS

Figure		Page
1	Angular Size as a Function of Contrast for a 99 Percent Probability (Confidence) and a Lack of Knowledge of Target Position of ± 4 Degrees or More	2
2	Douglas and Young (1945), Figure 8, Daytime Transmissometer Calibration, $\epsilon_v = C_r$	3
3	Middleton (1952), Figure 10.1, Frequency Distribution of Values of Threshold Contrast from 1000 Direct Observations at Ottawa	4
4	Ottawa Observations Regraphed as a Function of Attenuation Coefficient Times Sighting Range αr	4
5	Middleton (1952), Figure 10.2, Frequency Distribution of Values of Threshold Contrast Calculated from 285 Observations on Mount Washington, November 13, 1943 to April 21, 1944	4
6	Mount Washington Data Regraphed as a Function of Attenuation Coefficient Times Sighting Range αr	4
7	Hering, <i>et al.</i> (1971), Figure 9, Comparison Between Transmissometer Measurements and Human Visibility Observations During the Daytime, $\epsilon_v = C_r$	5
8	Relative Visual Range as a Function of Inherent Contrast and Inherent Target to Background Reflectance Ratio for a Contrast Threshold of 0.05	8
9	Relative Visual Range as a Function of Horizon Sky Equivalent Reflectance for Some Sample Target Reflectances	8
10a	Horizon Sky Reflectance Based Upon Modified Moon and Spencer Equation for an Overcast Sky	9
10b	Horizon Sky Reflectance Curves with Overlay of Relative Visual Range Curves for Sample Target Reflectances	9
10c	Illustration of Method of Use of Overlay Curves	10
11a	Horizon Sky Equivalent Reflectance from Low Altitude Airborne Measurements	11
11b	Horizon Sky Equivalent Reflectance from Low Altitude Airborne Measurements with Overlay of Relative Visual Range Curves for Sample Target Reflectances	11

DAYTIME VISIBILITY, A Conceptual Review*

Jacqueline I. Gordon

1. INTRODUCTION

Visibility is one of the standard meteorological parameters reported to summarize the state of the weather. These visibilities are primarily based on visual sightings by meteorologists at airports. These are often made hourly and are available for specific dates or as historical averages which summarize the state of the atmosphere at each locality. This report will attempt to define the psychophysical and physical bases of daytime visibility sightings and to correlate this daytime visibility with physical measurements of air clarity.

The World Meteorological Organization (WMO (1971) Sec. 10.1.1) defines daytime visibility as follows: "*Meteorological visibility by day is defined as the greatest distance at which a black object of suitable dimensions, situated near the ground, can be seen and recognized, when observed against a background of fog or sky.*" In order to understand the meaning of this visibility distance, let us review the pertinent psychophysical data on visual thresholds and the equations for determining the degradation of the luminance signal by the atmosphere.

2. VISUAL THRESHOLDS FOR DAYLIGHT ILLUMINATION

Visual thresholds for daylight are expressed in terms of the just perceptible apparent contrast of the object C_r against the background. The contrast is a function of the apparent object luminance ${}_rB_r$ and the apparent background luminance ${}_bB_r$,

$$C_r = \frac{{}_rB_r}{{}_bB_r} - 1. \quad (1)$$

The contrast threshold of the human eye for full daylight changes very little as a function of background luminance ${}_bB_r$, but is a strong function of the angular subtense of the target and the time spent looking at the target Δt . Figure 1 contains a graph of angular size as a function of contrast for confident sighting (99 percent

probability) and a lack of knowledge of target position of ± 4 degrees or more.

The data for long duration viewing $\Delta t = 24$ seconds— ∞ are from the Tiffany experiment, Blackwell (1946). The liminal contrast values (50 percent probability of detection) were multiplied by 1.91 to obtain a 99 percent probability and by 1.31 for lack of exact knowledge where to look (no orientation lights such as are used in the vision experiments). The total factor was $1.91 \times 1.31 = 2.50$. The Tiffany data are tabulated in Appendix A of Duntley (1946).

The data for 0.33 second viewing are from Taylor (1964). These forced-choice liminal contrasts were first multiplied by a factor of 1.2 to change from the Forced-Choice to a Yes-No situation. Thus the total factor used for the 0.33 second data was $1.2 \times 1.91 \times 1.31 = 3.00$.

The correction factors are taken from Taylor (1964).

The Tiffany $\Delta t = \infty$ data indicate that the horizon luminances for full daylight, clear or overcast (3400 to 340 $lu/\Omega m^2$) make very little difference to the threshold contrast except at very small angular size. The time used in viewing the object does have a direct effect on the threshold especially for large angular size objects. The 0.33 second viewing time is the average fixation time during free-search situations as determined by White (1964).

The WMO (1971) recommendation on object size is as follows: "*In order that day-time visibility measurements should be representative, they should be made using objects subtending an angle of not less than 0.5 degree at the observer's eye.*" Also they indicate that if instruments are used to evaluate the visibility by day, a contrast threshold of 0.025 should be used. Angular sizes in degrees are indicated on the second scale on the ordinate of Fig. 1. A contrast of 0.025 is indeed consistent with an angular size of 0.5 to 5 degrees for the 0.33 second curve in Fig. 1.

3. DEGRADATION OF THE LUMINANCE SIGNAL BY THE ATMOSPHERE

The apparent contrast of an object $C_r(z, \theta, \phi)$ is a function of the inherent contrast $C_o(z, \theta, \phi)$, the inherent background luminance ${}_bB_o(z, \theta, \phi)$, the apparent

* The first draft of this review was issued as Visibility Laboratory Technical Memorandum AV78-071t, 21 July 1978.

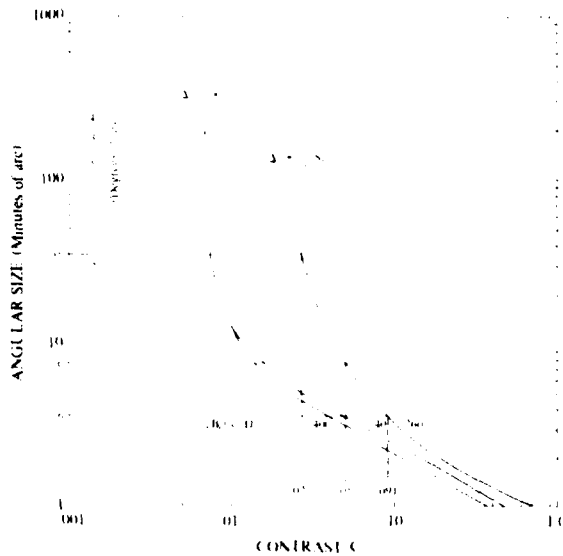


Fig. 1 Angular Size as a Function of Contrast for a 99 Percent Probability (Confidence) and a Lack of Knowledge of Target Position of ± 4 Degrees or More

background luminance ${}_bB_r(z, \theta, \phi)$ and the luminance transmittance of the intervening atmosphere $T_r(z, \theta)$,

$$C_r(z, \theta, \phi) = C_o(z, \theta, \phi) \frac{{}_bB_o(z, \theta, \phi)}{{}_bB_r(z, \theta, \phi)} T_r(z, \theta). \quad (2)$$

The modifiers in parenthesis refer to the altitude z of the sensor, zenith angle θ and azimuth ϕ of the path of sight (z_o refers to the altitude of the object). Equation (2) is rigorously true for monochromatic radiation, however it may also be used as a reasonable engineering approximation for sensors with a broad passband in the visible portion of the spectrum.

Since the WMO (1971) specifies a black object viewed against a horizon sky, and since the inherent contrast of a black object is reasonably close to -1, Eq. (2) can be further simplified. If the horizon sky is further restricted to mean the "cloudless" horizon sky, the ratio of inherent to apparent background luminance also equals 1. Now Eq. (2) can be rewritten as:

$$|C_r(0, 90^\circ, \phi)| = T_r(0, 90^\circ). \quad (3)$$

The absolute value of the apparent contrast is used in Eq. (3) since the transmittance is a positive term and since the visual threshold depends upon the absolute value of apparent contrast and not on whether the contrast is positive or negative.

The transmittance at range r can be also expressed as a function of the attenuation coefficient $\alpha(z)$ and the range r ,

$$C_r(0, 90^\circ, \phi) = e^{-\alpha(0)r} \quad (4)$$

The attenuation coefficient $\alpha(0)$ is the average attenuation coefficient for the photically filtered sensor over the path length r . If the layer of atmosphere near the ground is homogeneous, $\alpha(0)$ is isotropic and can be measured as a point function and applied to the total path.

Thus Eq. (4) defines the visibility range r once the contrast threshold $|C_r|$ is also defined.

4. THRESHOLD CONTRAST OF VISIBILITY TARGETS

The question that arises at this point is, what threshold contrast is actually limiting the visibility when a target is sighted. Fortunately, a number of experiments have been conducted wherein the visibility range was determined visually at the same time as the degradation of the atmosphere was measured with physical instruments.

One of the best experiments attempting to measure threshold contrast for visibility targets was conducted by Douglas and Young (1945). They measured transmittance in terms of the transmittance to a unit distance of 1 kilometer, i.e.:

$$T_r(0, 90^\circ) = T_1(0, 90^\circ)^r, \quad (5)$$

where r is expressed in kilometers. Thus the contrast threshold can be expressed as

$$|C_r(0, 90^\circ, \phi)| = T_1(0, 90^\circ)^r. \quad (6)$$

They measured the transmittance with a transmissometer and also determined the visibility range r using black panels viewed against the horizon sky for short distances. In addition, they used some supplementary non-black targets against the horizon sky at longer distances (with some overlap in range). Equation (6) can be rewritten as

$$-\log[-\log T_1(0, 90^\circ)] = +\log r - \log[-\log |C_r|]. \quad (7)$$

Equation (7) is in the classical form of an equation for a straight line, $y = mx + b$. The Douglas and Young Fig. 8, which is a data graph in the form of $-\log[-\log T_1(0, 90^\circ)]$ versus $\log r$, is reproduced herein as Fig. 2. The scales are marked in transmission per kilometer T_1 and visual range r . If there is a reasonably constant threshold contrast $|C_r|$, the data will result in a straight line on the graph, with a slope of 1 or 45 degrees. The intercept $-\log[-\log |C_r|] = -\log(-\log T_1)$ is at the point $\log r = 0$, thus $|C_r| = T_1$ when $r = 1$. They computed the average $|C_r| = 0.055$ from Eq. (7) using the data for the black panels (Grades A, B & C) and the miscellaneous targets, but ignored the twilight and weather bureau data. The black panel data fit the average best. No statistical measure of deviation was given.

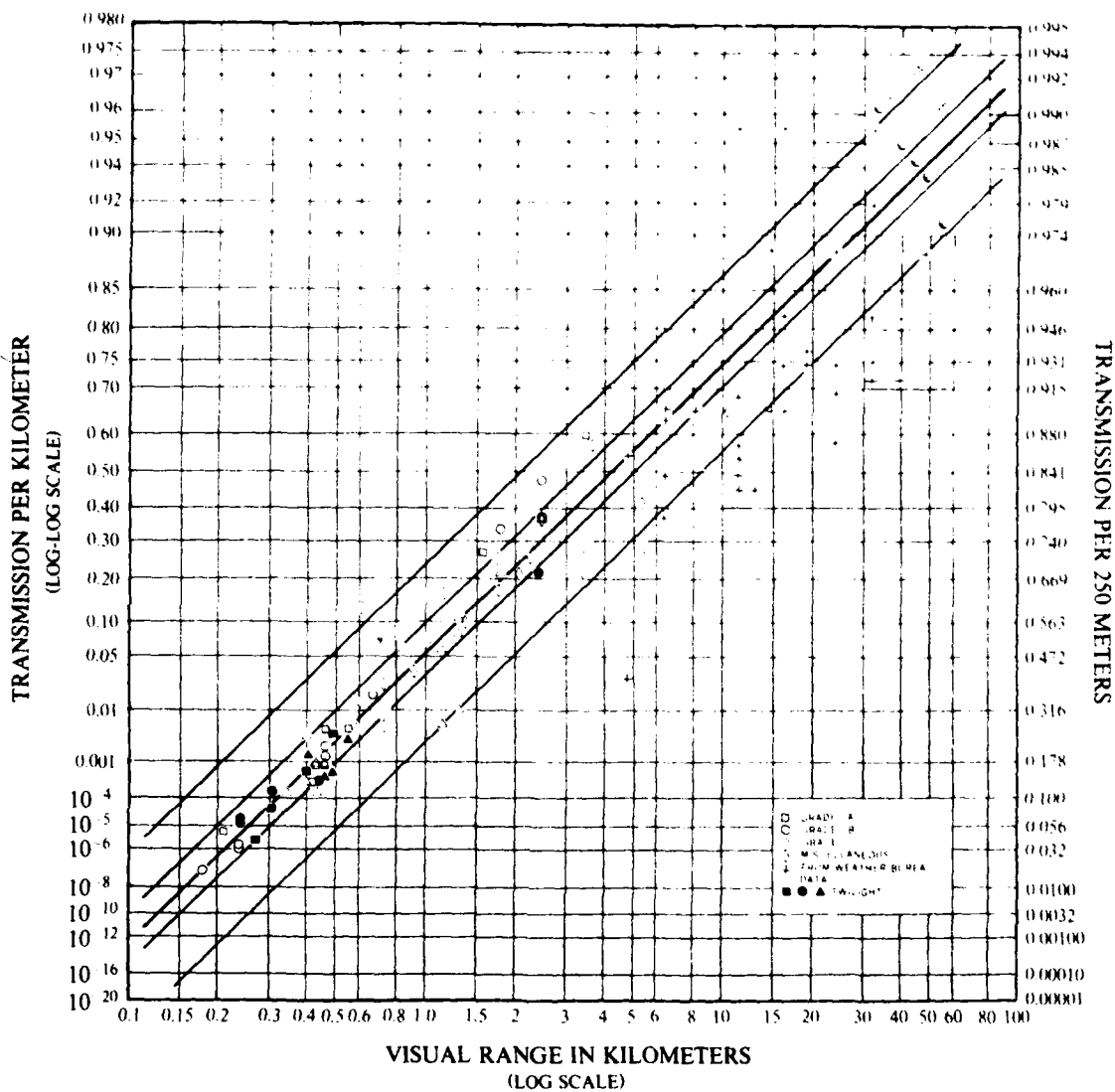


Fig. 2 Douglas and Young (1945), Figure 8. Daytime Transmissometer Calibration. $\epsilon_a = C_r$

If the threshold contrast is a constant, the product of the attenuation coefficient times the sighting range αr is also a constant, i.e., another way of expressing Eq. (4) is

$$-\ln |C_r| = \alpha r. \quad (8)$$

The product αr based on the average $|C_r|$ for the Douglas and Young data was 2.9.

Duntley (1948) reported a comparison of the visibility as reported by a staff meteorologist at Tiffany and the meteorological range as calculated from measurements of the luminance transmittance. On the average, the visibility range was 0.75 of the meteorological range. The meteorological range MR was defined by a threshold contrast of 0.02 or $r/\text{MR} = 3.9$. If the visibility r is 0.75 of

the meteorological range MR, $\alpha r = 0.75(3.9) = 2.9$ and $C_r = 0.055$. This is in good agreement with the Douglas and Young (1945) values.

Middleton (1952) cited two other experiments to obtain $|C_r|$. One in Ottawa during 1950-1951 measured the apparent contrast of visibility targets against a horizon background at the moment of use to specify visibility range. These apparent contrasts are graphed in Fig. 3 (Middleton's Fig. 10.1). I computed an average $|C_r| = 0.042$ and a standard deviation of 0.031. The average αr for the Ottawa data based on Eq. (8) is 3.2.

In order to get a better picture of the variability of the αr product, I regraphed Fig. 3 by computing αr and the number per $\Delta|\alpha r|$ for each $\Delta C_r = 0.01$ interval. This graph is given in Fig. 4. The $|C_r|$ interval 0-0.01 was approximated by $C_r = 0.001-0.01$.

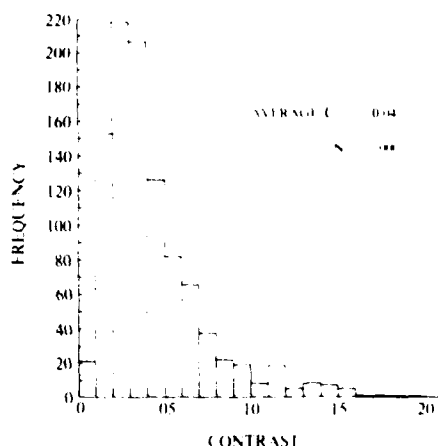


Fig. 3 Middleton (1952), Figure 10.1, Frequency Distribution of Values of Threshold Contrast from 1000 Direct Observations at Ottawa

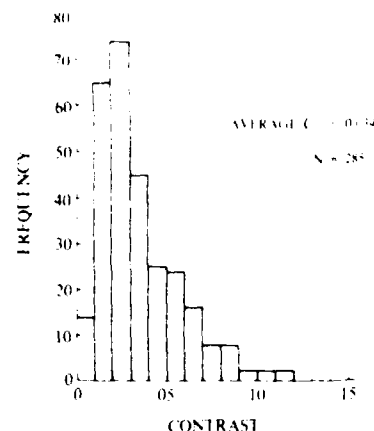


Fig. 5 Middleton (1952), Figure 10.2, Frequency Distribution of Values of Threshold Contrast Calculated from 285 Observations on Mount Washington, November 13, 1943 to April 21, 1944

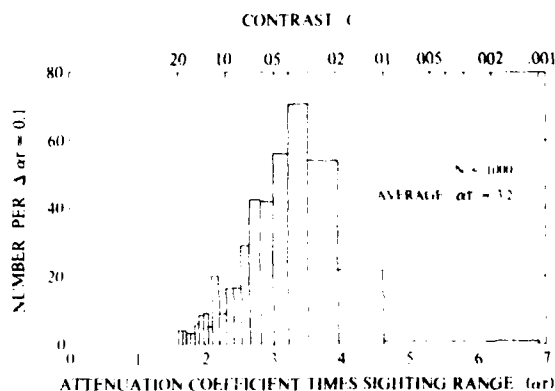


Fig. 4 Ottawa Observations Regraphed as a Function of Attenuation Coefficient Times Sighting Range ar

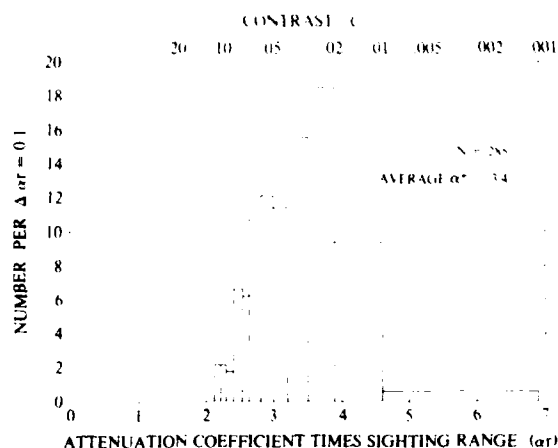


Fig. 6 Mount Washington Data Regraphed as a Function of Attenuation Coefficient Times Sighting Range ar

The second experiment cited by Middleton used 1943-1944 Mount Washington data on measured attenuation coefficient and visibility ranges to compute $|C|$ (presumably from Eq. (4)). These apparent contrasts are graphed in Fig. 5 (Middleton's Fig. 10.2). I computed the average $|C| = 0.034$ with a standard deviation of 0.022. The average ar based on Eq. (8) is 3.4. The method of obtaining the visibility range in cloud was unspecified. These data are regraphed as a function of ar and the number per $\Delta ar = 0.1$ in Fig. 6.

Horvath and Noll (1969) reported measurements of total volume scattering coefficient $s(0)$ and concurrent visibility ranges for two observers on the roof of a four story building in Seattle. The total volume scattering coefficient was measured with an integrating nephelometer, an instrument described in full by Charlson, *et al.* (1967). The total scattering coefficient is equivalent to the attenuation coefficient $\alpha(0)$ if there is no

absorption. The observers reported the prevailing visibility based on visibility markers consisting of large buildings and mountain ridges at known distances. The prevailing visibility was defined as "the greatest visibility attained or surpassed around at least half of the horizon circle but not necessarily in continuous sections."

Horvath and Noll (1969) indicated that visibilities from the first observer resulted in an average ar of 3.5 ± 0.36 from 34 observations. The second observer made 33 observations and had an average ar of 3.18 ± 0.25 . The two observers made no simultaneous observations.

Hering, *et al.* (1971) reported concurrent measurements of transmittance and visibility or sighting range r during periods of summer fog. The sighting ranges were determined for distances up to 0.5 mile by the use of black rectangular targets with horizon sky

backgrounds spaced at 0.0625 mile intervals resulting in 8 targets in the 0.5 mile range. The size of the targets was increased with distance so as to subtend 0.5 degree at each distance. Antenna towers were used as visibility markers for distances greater than 0.5 mile. The measurements, both in transmittance and sighting range, were 1-minute averages.

Equation (8) may be rewritten as

$$\log r = -\log \alpha + \log(-\ln|C_t|) \quad (9)$$

Again if the threshold contrast $|C_t|$ is constant, a graph of $\log r$ (or \log visibility) as a function of $\log \alpha$ will result in a straight line with a slope of -1. Fig. 9 from Hering, *et al.* (1971) is in this form, it is reproduced as Fig. 7 herein. The solid line represents a contrast threshold of 0.02 and the dashed line a contrast threshold of 0.055. The black targets (visibilities ≤ 0.5 mile) yielded sighting ranges consistent with 0.02 and the use of the antenna towers resulted in higher threshold contrasts, nearer to or greater than 0.055. The lines are for interpreting the data but were not derived from the data.

The results of the six studies described above are summarized in Table 1.

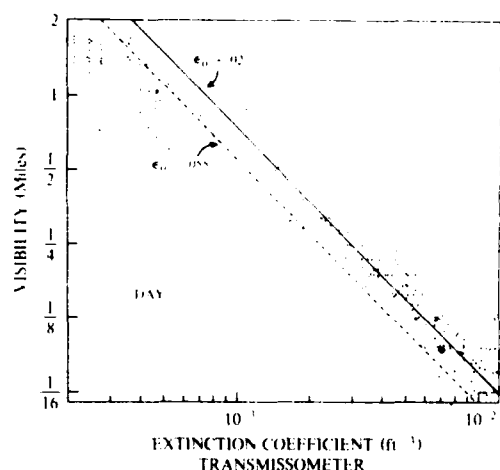


Fig. 7. Hering, *et al.* (1971), Figure 9, Comparison Between Transmissometer Measurements and Human Visibility Observations During the Daytime, $\epsilon_a = C_t$.

5. THRESHOLD ANGULAR SIZE OF VISIBILITY OBJECTS

Although the WMO (1971) and Middleton (1952) advise the use of visibility objects subtending an angle of 0.5 to 5 degrees, the evidence from the studies just described indicates the actual use of visibility objects of smaller angular size.

Douglas and Young (1945) indicated that, at the visibility range distances, the black panels varied from 3 to 28 minutes of arc in angular size. These angles correspond to contrasts of 0.029 to 0.11 on the 0.33 second curve in Fig. 1. The lines for $C_t = \epsilon_a = 0.098$ and 0.031 in Fig. 2 indicate that the bulk of the black panel data fall in that contrast range. This range is practically synonymous with the range indicated by the 0.33 second curve based on the actual α range for the experiment. Thus the Taylor (1964) 0.33 second data for full daylight, with a correction factor of 3 to allow for 99 percent probability of detection and lack of knowledge of target position of ± 4 degrees or more, are consistent with the visibility range experiment conducted by Douglas and Young (1945).

The two experiments cited by Middleton (1952) did not measure target angular size.

The Ottawa data cited by Middleton on contrast measured during visibility range sightings yielded an average threshold contrast of 0.042 and a standard deviation of 0.031 or a range for 67 percent of the cases of 0.011 to 0.073 in contrast. The corresponding angular size range based upon the 0.33 second curve in Fig. 1 is 4.5 to >120 minutes of arc for this contrast range, and 10 minutes of arc for the average contrast value.

The Mount Washington data based on attenuation coefficients measured during the visibility range sightings, yielded an average contrast of 0.034 and a standard deviation of 0.022 or a range of 0.012 to 0.056 contrast for 67 percent of the cases. The corresponding angular size range based on the 0.33 second curve in Fig. 1 is 6.3 to >120 minutes and the average is 20 minutes.

The smaller contrast values (0.011 and 0.012) at the lower end of the ranges for one standard deviation actually indicate a probable larger time interval for the sightings rather than a larger angular size than 120 minutes. In other words, a vision curve somewhere between $\Delta t = \infty$ and $\Delta t = 0.33$ seconds probably is appropriate for those low

Table 1.

Threshold Contrast and the Attenuation Coefficient Times the Sighting Range αr for Daytime Visibilities

Reference	Description	Threshold Contrast		Attenuation Coefficient x Sighting range αr
		Average	Standard Deviation	
Douglas & Young (1945)	Transmissometer	0.055		2.9
Duntley (1948)	Tiffany	0.055		2.9
Middleton (1952)	Mt. Washington (1943-44)	0.034	0.022	3.4
Middleton (1952)	Ottawa (1950-51)	0.042	0.031	3.2
Horvath & Noll (1969)	Observer I	0.030		3.5 ± 0.36
Horvath & Noll (1969)	Observer II	0.042		3.2 ± 0.25
Hering <i>et al.</i> (1971)	Black targets ($\leq 1/2$ mi Visibility)	≥ 0.02		≥ 3.9
Hering <i>et al.</i> (1971)	Antenna towers ($> 1/2$ mi Visibility)	≥ 0.055		≤ 2.9

contrasts. A change in the confidence limits, even to a probability of 50 percent does not allow for a large enough contrast factor between the contrast for 120 minutes of arc and the 0.011 or 0.012 contrast.

On the other hand, one must posit an untrained observer before it is reasonable to depict a vision curve to the right of the 0.33 second curve. Therefore, I believe it is more likely that many of the visibility targets were indeed less than 0.5 degrees during the sightings and hence the average angular sizes were indeed less than 0.5 degrees for both studies cited by Middleton (1952).

Horvath and Noll (1969) measured total volume scattering coefficient (which is reasonable to assume equivalent to the attenuation coefficient) and obtained the sighting range r simultaneously. The average attenuation coefficient times sighting distance for Observer I was 3.5 ± 0.36 . The resultant average contrast computed from Eq. (4) is 0.03 with a range of 0.021 to 0.043 in contrast. The corresponding angular size average is 24 minutes with a range of 10 to >120 minutes of arc based on the 0.33 second curve in Fig. 1. Similarly the average attenuation coefficient times sighting distance for Observer II was 3.2 ± 0.25 . The computed average contrast is 0.042 and the computed contrast range is 0.032 to 0.052. The corresponding angular size average is 10 minutes of arc with a range of 6.7 to 20 minutes of arc.

The Hering, *et al.* (1971) black target data were for 30 minutes (or 0.5 degree) angular subtense. The

approximate threshold contrast of 0.02 is not inconsistent with Fig. 1 in that sighting ranges were for a 1 minute period, but were considered an average over that period rather than the best distance possible during 1 minute. A vision curve slightly to the left of the 0.33 second curve is probably not inappropriate for such data.

The longer sighting ranges obtained using antenna towers as targets undoubtedly indicate the targets were at a smaller angular subtense than 30 minutes. The 0.33 second curve indicates an average subtense of 6.5 minutes for a contrast threshold of 0.055, thus a curve slightly to the left would indicate targets <6.5 minutes in size.

The contrast and angular size relationships just described are summarized in Table 2. The average angular size of the visibility targets except for the Hering, *et al.* (1971) black targets was always less than 0.5 degrees, ranging from 6.5 minutes for the Douglas and Young (1945) and Hering, *et al.* (1971) antenna targets experiment to 24 minutes for Observer I in the Horvath and Noll (1969) study. Indeed, this is not entirely surprising since for a visibility target to be 0.5 degree or larger, it would have to be equal to or greater than the angular size of the sun or moon.

Thus although the WMO (1971) recommends a target 0.5 degree or greater in size, the corresponding use of a threshold contrast of 0.025 and thus the attenuation coefficient range product of 3.7, the historical visibility data do not actually conform to this recommendation.

Table 2.
The Contrast and Angular Size Relationship Based Upon 0.33 Second, a 99 Percent Probability,
and a Lack of Knowledge of Target Position of ± 4 Degrees or More

Reference	Basis	Average or Range	Contrast C_r	Angular Size (Minutes of Arc)
Douglas & Young (1945)	Measured Transmittance	Average	0.055	6.5
	Measured Angular Size	Min	0.11	3
		Max	0.029	28
Duntley (1948)	Measured Transmittance	Average	0.055	6.5
Middleton (1952) Ottawa	Measured Contrast	Average	0.042	10
		+1 STD C_r	0.073	4.5
		-1 STD C_r	0.011	>120 or $\Delta t > 0.33$ sec
Mount Washington	Measured Attenuation Coefficient	Average	0.034	20
		+1 STD C_r	0.056	6.3
		-1 STD C_r	0.012	>120 or $\Delta t > 0.33$ sec
Horvath & Noll (1969) Observer I	Measured Scattering Coefficient	Average	0.030	24
		-0.36 σ_r	0.043	10
		+0.36 σ_r	0.021	>120 or $\Delta t > 0.33$ sec
Observer II	Measured Scattering Coefficient	Average	0.042	10
		-0.25 σ_r	0.052	6.7
		+0.25 σ_r	0.032	20
Hering <i>et al.</i> (1971) Black Targets	Measured Transmittance and Measured Angular Size	Average	0.020	30
Antenna Towers	Measured Transmittance	Average	≥ 0.055	< 6.5

6. RELATIONSHIP OF ATTENUATION COEFFICIENT AND THRESHOLD SIGHTING RANGE

The attenuation coefficient is related to the threshold sighting range and threshold contrast according to Eq. (8). A threshold contrast of 0.05 results in an attenuation coefficient times threshold sighting range of 3.0. Allowing a 20 percent range for variability in sighting distance results in an αr range of 2.4 to 3.6 or

$$\alpha r = 3 \pm 0.6. \quad (10)$$

The corresponding threshold contrast range is 0.027 to 0.091. This range of threshold values of contrast and attenuation coefficient times sighting range includes the bulk of the best defined data, Grades A, B & C from Douglas and Young (1945). [This range is very close to the lines drawn for $C_t = 0.098$ and 0.031 in Fig. 2.]

As can be seen from Table 1, this threshold value and range of ± 20 percent for αr also includes the average values from Duntley (1945), the average from the two experiments cited by Middleton (1952), the average for each observer from Horvath and Noll (1969), and the antenna target data of Hering, *et al.* (1971). [The ± 20 percent range actually includes 60 percent of the Ottawa data and 52 percent of the Mount Washington data].

In a way this is remarkable consistency considering the variability of the values recommended historically. The various values of recommended threshold contrast as summarized by Middleton (1952) are given in the third column of Table 3. The corresponding αr using Eq. (8) are given in Col. 4.

Table 3.

Historical Summary of Previously Recommended Threshold Values

Reference	Description	Threshold Contrast	Attenuation Coefficient Times Threshold Range
Koschmieder (1924)	Non-Experimental	0.02	3.9
Houghton (1939)	Fog	0.06	2.8
Schallenger & Little (1940)	Haze & Smoke	0.032	3.4
Bricard (1944)	Fog	0.0077	4.9
		0.025	3.7
Barteneva (1960)	Visibility	0.05	3.0
WMO (1971)	MOR	0.05	3.0

There are several more recent recommendations for visibility threshold values which are consistent with Eq. (10). These are also given in Table 3. Barteneva (1960) used an αr of 3 to compare her measured values of transmittance and total volume scattering coefficient to the visibility.

The WMO (1971) recommended (as of 1957) the adoption of the concept of Meteorological Optical Range (MOR) which is defined as: "The length of path in the atmosphere required to reduce the luminous flux in a collimated beam from an incandescent lamp at a colour temperature of 2700°K to 0.05 of its original value, the luminous flux being evaluated by means of the photopic luminosity function of the CIE." This corresponds to an $\alpha r = 3$.

The Visibility Laboratory has also been using $\alpha r = 3$ (Duntley, *et al.* (1972) and ensuing reports) as an approximation of the Douglas and Young (1945) data.

The contrast threshold 0.05 and the contrast range 0.027 to 0.091 which correspond to the ± 20 percent range in sighting distance specified by Eq. (10) are depicted in Fig. 1 as dashed lines connecting the abscissa to the 0.33 second visual threshold curve which in turn connects them to the corresponding dashed lines on the ordinate indicating threshold angular size. The threshold angular size is thus 7.6 minutes of arc with a range from 3.6 to 35 minutes of arc corresponding to the ± 20 percent range in sighting distance.

Thus the visibility can be reasonably defined as the distance a black target can be seen against the cloudless horizon sky. It is related to the attenuation coefficient with an accuracy of ± 20 percent by the relationship indicated by Eq. (10).

Awareness that the visibility distance and attenuation coefficient are most closely related to a 0.33 second fixation time and an angular target size of 7.6 minutes would undoubtedly increase the precision level of the visibility sightings.

The errors in making visibility estimates using non-black targets and/or backgrounds other than the horizon sky can now be evaluated with reference to the relationship defined by Eq. (10).

7. RELATIVE VISUAL RANGE OF NON-BLACK TARGETS

The visual range r_1 of a non-black target as seen against the cloudless horizon sky is:

$$r_1 = \alpha(0)^{-1} [\ln(C_0) - \ln(C_1)] \quad (11)$$

Whereas the visual range of a black target is

$$r = \alpha(0)^{-1} [-\ln(C_t)] \quad (12)$$

Dividing Eq. (11) by Eq. (12) we get the visual range of a non-black target relative to the visual range based on a black target. Then since the contrast threshold of a non-black target is equivalent to the contrast threshold of a black target $|C_t| = |C_1|$, we have

$$\frac{r_1}{r} = \frac{\ln(C_0) - \ln(C_1)}{-\ln(C_t)} = \frac{\ln(C_0)}{3} + 1 \quad (13)$$

Eq. (13) is a measure of the error of using a non-black target assuming the contrast threshold for the visibility target to be 0.05. The absolute value of inherent contrast is used in Eq. (13) since the visual threshold depends on the absolute value but not whether the contrast is positive or negative. Also, the natural logarithm cannot be evaluated for a negative value of contrast.

Inherent contrast can be expressed as a function of the target to background reflectance ratio.

$$C_o = \frac{tR_o}{bR_o} - 1 \quad (14)$$

The relative visual range was evaluated for various values of inherent target to background reflectance ratio and graphed in Fig. 8. The lower scale on the abscissa gives the reflectance ratio, and the upper scale is marked in contrast. The ordinate is marked in relative visual range. The relative visual range stays between 1 and 0.95 for negative contrasts from -1 to -0.86 which corresponds to a range in target to background ratio of 0 to 0.14. For positive contrasts the relative visual range changes rapidly with the target to background ratio. There is only a brief range of target to background ratios of 1.86 to 2.16 when the relative visual range is 1.0 ± 5 percent for positive contrast targets.

Horizon Sky Equivalent Reflectance.

It is useful to have an equivalent reflectance for the horizon sky so that contrasts of non-self luminous targets

of known reflectance can be evaluated as to contrast. The equivalent reflectance of the horizon sky would be

$$bR_o(0, 90, \phi) = \frac{N(0, 90^\circ, \phi) \pi}{H(0, 90^\circ, \phi + 180^\circ)} \quad (15)$$

The irradiance notation $H(0, 90^\circ, \phi + 180^\circ)$ indicates the altitude, zenith angle and azimuth of the normal from the surface of the irradiator.

The relative visual range can be graphed as a function of horizon sky reflectance for a given target reflectance. Curves for target reflectances 0.04 for black or forest, 0.10 for growing crops, 0.20 for sand, and 0.80 for white or snow are given in Fig. 9. This graph is essentially the inverse of Fig. 8 with the zero contrast point at the horizon sky reflectance value equal to the target reflectance.

As can be seen, with high sky reflectances greater than 1, a number of targets in addition to the black target,

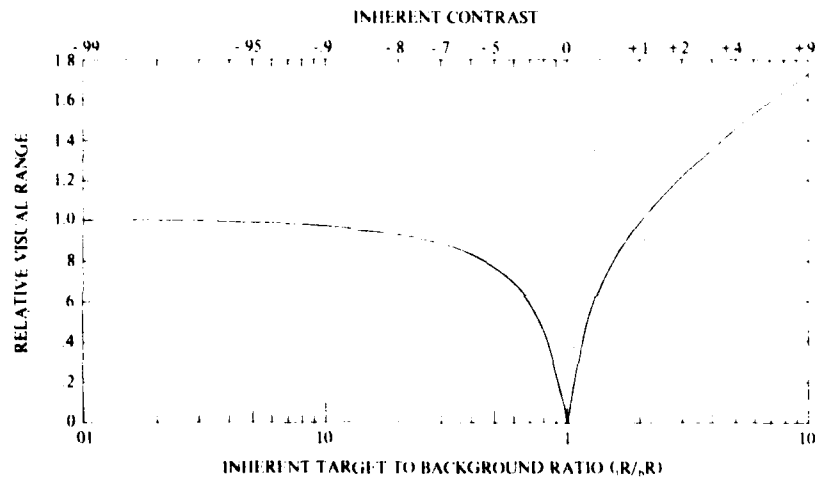


Fig. 8 Relative Visual Range as a Function of Inherent Contrast and Inherent Target to Background Reflectance Ratio for a Contrast Threshold of 0.05.

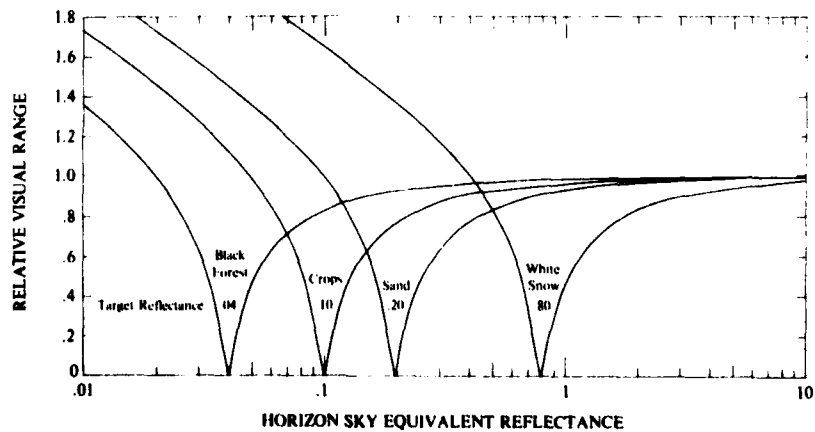


Fig. 9. Relative Visual Range as a Function of Horizon Sky Equivalent Reflectance for Some Sample Target Reflectances.

can be used to obtain visual range with reasonable accuracy.

Horizon Sky Reflectance for Overcast.

Middleton (1952) used a modified form of the Moon and Spencer (1942) equation for the overcast sky radiance as follows

$$N(0, \theta) = N(0, 90^\circ) [1 + m \cos \theta] \quad (16)$$

This relates the sky radiance at each zenith angle θ to the horizon sky radiance and assumes no azimuth dependency. The equivalent horizon sky reflectance based on Eq. (16) is

$$R(0, 90^\circ) = [0.5 (1+A) + \frac{m}{3} (\frac{2}{\pi} + A)]^{-1} \quad (17)$$

where A is the albedo.

Equation (17) is derived in the Appendix. The horizon sky reflectance based on Eq. (17) is graphed in Fig. 10a for various values of m as a function of albedo A. The albedo is the ratio of upwelling to downwelling illuminance. The ordinate is marked on the left side in horizon sky reflectance. On the right hand scale are noted

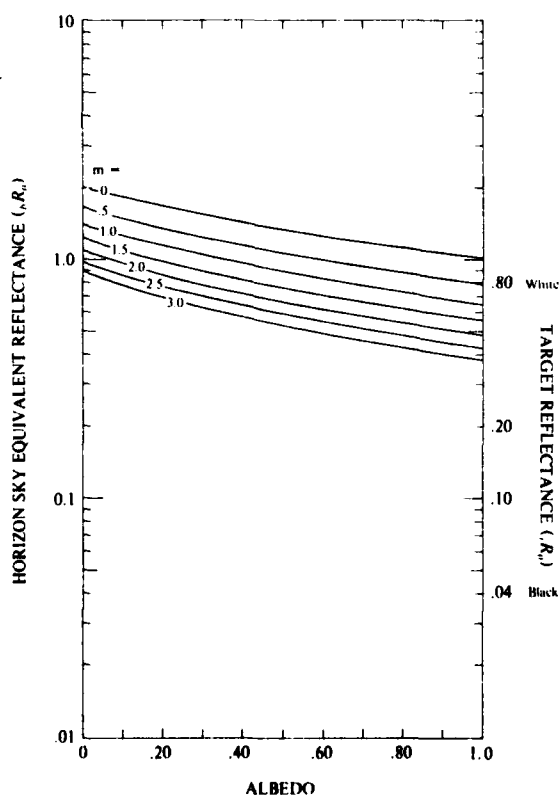


Fig. 10a. Horizon Sky Reflectance Based Upon Modified Moon and Spencer Equation for an Overcast Sky.

various target reflectances from black or 0.04 to white or 0.80. This graph can be interpreted in terms of the relative visual range by overlaying Fig. 9 on Fig. 10a, as shown in Fig. 10b. Figure 10c illustrates interpretation of the overlay as described in the figure caption.

As can be seen, the black target stays always at relative visual range ratios near 1.0, but a white target changes from negative to positive contrast depending on the albedo and value of m , and hence is not desirable as a visibility target.

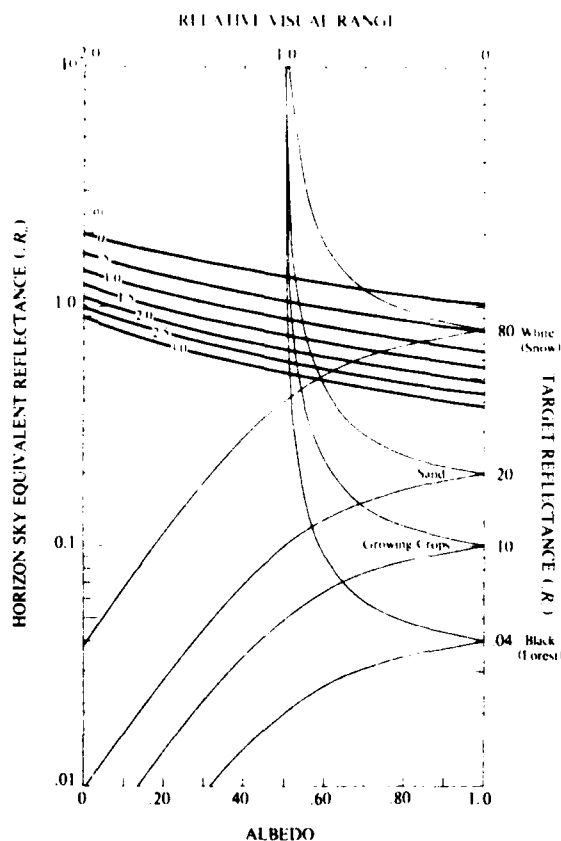


Fig. 10b. Horizon Sky Reflectance Curves with Overlay of Relative Visual Range Curves for Sample Target Reflectances.

Figure 10b is interpreted by using the horizontal leg of a right triangle to connect the point on the Horizon Sky Reflectance curve to the Target curve and then by using the vertical leg of the triangle to go from the Target curve to the appropriate Relative Visual Range scale indicated at the top of the graph. This is illustrated in Figure 10c for a horizon sky reflectance of 0.38 (appropriate for an m of 3.0 and an albedo of 1.0) and the black target; the resultant relative visual range is 0.96.

Horizon Sky Reflectance from 4π Radiance Measurements.

We have a few sample horizon sky reflectance values from actual measurements of sky and terrain radiance. A simple computer program MODE3, takes the values of upper and lower hemisphere luminance from

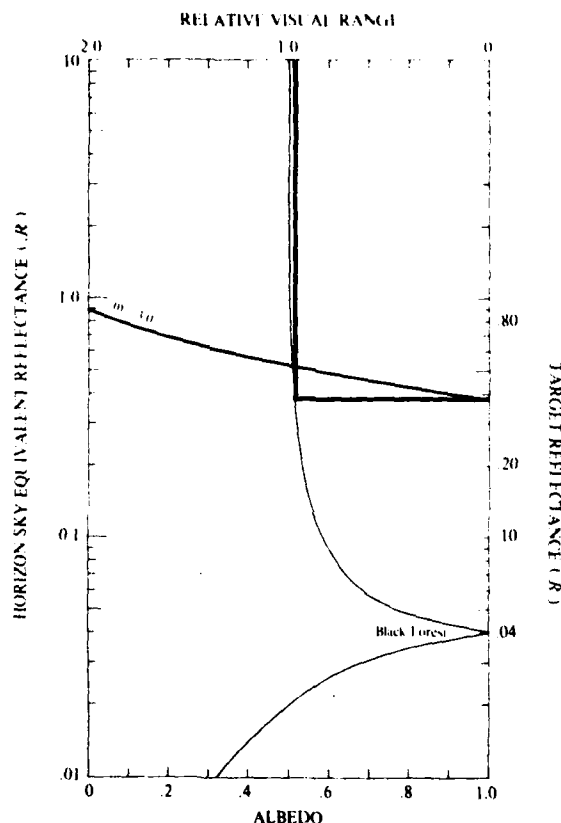


Fig. 10c. Illustration of Method of Use of Overlay Curves.

airborne scanner data arrays, and computes illuminance on a surface or surfaces specified by the zenith angle and azimuth of the normal from the surface. This program was run for illustrative purposes on low altitude data for an overcast day and for a separate problem for a cloudy day with unobscured sun. The sample values of horizon sky equivalent reflectance are graphed in Fig. 11a as a function of azimuth from sun.

The overcast day was on 25 May 1970 near Memmingen, Germany during the HAVENVIEW I field trip reported in Duntley, *et al.* (1972). The terrain was heavily cultivated, rolling pasture land occasionally interrupted by large patches of dark forest and had an albedo of 0.07. These reflectances are tabulated in Table 4. The values for horizon sky luminance are given in Col. 4 in units of $lu/\Omega m^2$. These are the same units used for adaptation or background level for Fig. 1.

The cloudy day data with unobscured sun are for 14 June 1973 near Meppen, Germany during the HAVENVIEW II field trip reported in Duntley, *et al.* (1976). The terrain consisted of mainly cultivated farmlands interspersed with dark patches of dense woods and had an albedo of 0.075 at the lowest airborne altitude.

The range of adaptation level (Col. 4 Table 4) is $5.50E3$ to $1.94E4$ $lu/\Omega m^2$. The Tiffany data curves ($\Delta r = \infty$) Fig. 1 are for $3.4E3$ and $3.40E2$ $lu/\Omega m^2$ respectively and the Taylor 0.33 second data for $2.60E2$ $lu/\Omega m^2$. It is assumed that the contrast threshold remains a constant at these high background luminance levels and is not degraded by glare.

From overlaying Fig. 9 on Fig. 11a, as depicted in Fig. 11b, we see that the black target, reflectance 0.04, still yields a relative visual range of 0.95 for even the lowest horizon sky equivalent reflectance of 0.30 which was at 180 degrees azimuth for the cloudy sky. The overcast horizon sky reflectances are very azimuth dependent and the cloudy sky values even more so. Non-black targets such as a grass covered mountain ($R_o = 0.10$ estimated) can be used with reasonable accuracy for azimuths $0-90^\circ$ but are more error prone near 180° azimuth. A snow covered mountain should never be used (estimated reflectance 0.80).

These horizon sky equivalent reflectances are limited to terrains with albedos near 0.07 and to a medium high sun, sun zenith angles 39 to 52 degrees. It would be extremely interesting to have values of horizon reflectance for clear skies, a range of sun zenith angle and albedo, etc.

Table 4.

Equivalent Horizon Sky Reflectances from Low Altitude Airborne Measurements for Pseudo-Photopic Filter
Mean Wavelength 557 Nanometers

Flight No.	Altitude (m)	Path of Sight from Sun ϕ	Sky Luminance ($lu/\Omega m^2$) $B_{\infty}^*(z, 90, \phi)$	Illuminance (lu/m^2) $E(z, 90, \phi + 180)$	Horizon Sky Equivalent Reflectance $R_o(z, 90, \phi)$	Albedo	Sun Zenith Angle	Description
C-289	258	0	1.55E4	1.04E4	4.67	.075	40.5	Scattered clouds, unobscured sun
		90	8.89E3	1.44E4	1.93			
		180	7.47E3	7.94E4	297			
C-289	1192	0	1.95E4	1.45E4	4.22	.071	39.1	Broken clouds, unobscured sun
		90	1.17E4	2.05E4	1.80			
		180	9.37E3	8.66E4	340			
C-134	280	0	9.52E3	1.45E4	2.06	.070	51.6	Overcast
		45	7.48E3	1.49E4	1.58			
		90	6.39E3	1.95E4	1.03			
		135	6.50E3	3.80E4	538			
		180	6.15E3	4.64E4	417			
		-135	5.98E3	3.77E4	498			
		-90	5.50E3	2.00E4	862			
		-45	7.43E3	1.59E4	1.47			

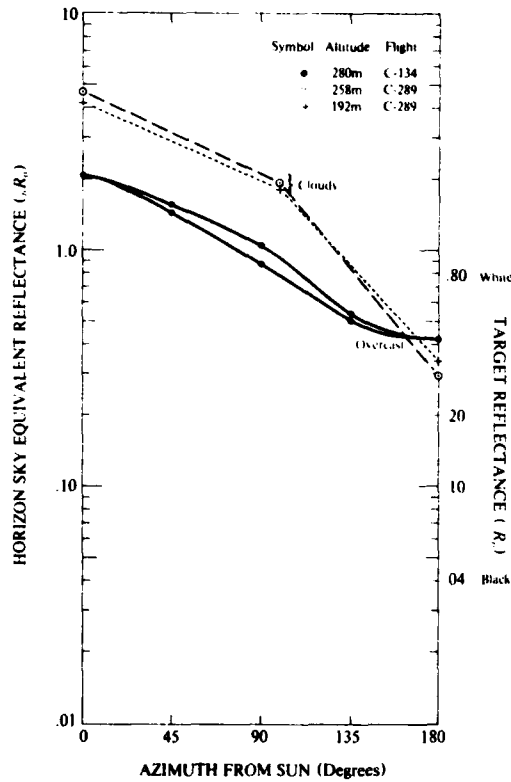


Fig. 11a Horizon Sky Equivalent Reflectance from Low Altitude Airborne Measurements

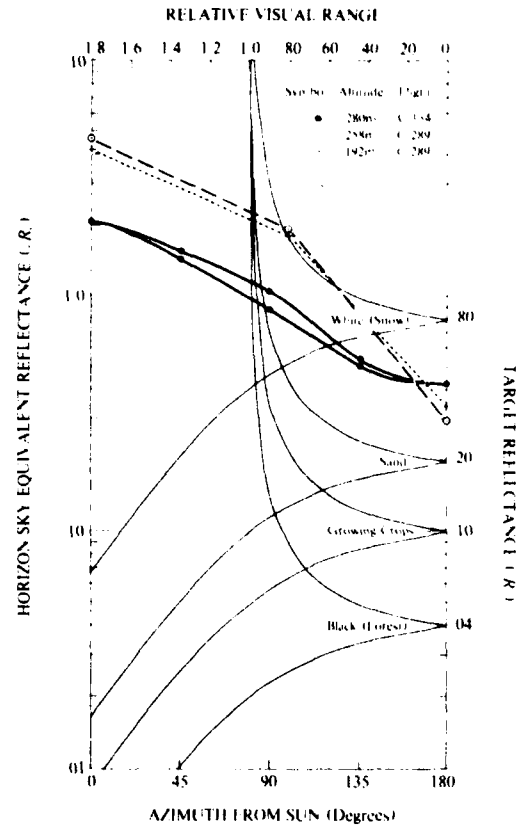


Fig. 11b Horizon Sky Equivalent Reflectance from Low Altitude Airborne Measurements with Overlay of Relative Visual Range Curves for Sample Target Reflectances

8. BACKGROUNDS OTHER THAN THE CLEAR HORIZON SKY

The threshold contrast of a black target seen against the clear horizon sky is a function of the transmittance at the visual range r ,

$$|C_r| = T_r. \quad (18)$$

The apparent contrast of a black target against any background at distance r_2 is

$$|C_{r_2}| = \frac{bN_o}{bN_{r_2}} T_{r_2}. \quad (19)$$

If the target is seen against a background which is behind the target at distance $n'r$ from the observer, the apparent radiance of the background bN_{r_2} as measured at the observer is,

$$bN_{r_2} = bR_o \frac{H}{\pi} T_r^n + R_q \frac{H}{\pi} (1 - T_r^n). \quad (20)$$

where bR_o is the background reflectance and R_q is the equilibrium reflectance. Similarly, if the target is at distance $n'r$ from the observer, the radiance of the background as measured at the target position bN_o is

$$bN_o = bR_o \frac{H}{\pi} T_r^{n-n'} + R_q \frac{H}{\pi} (1 - T_r^{n-n'}). \quad (21)$$

Also the transmittance T_{r_2} in terms of the threshold range r is

$$T_{r_2} = T_r^{n'}. \quad (22)$$

Now substituting Eqs. (20), (21), and (22), into Eq. (19), we get

$$|C_{r_2}| = \frac{[bR_o T_r^{n-n'} + R_q (1 - T_r^{n-n'})] T_r^{n'}}{bR_o T_r^n + R_q (1 - T_r^n)}. \quad (23)$$

Now we want to put the observer at the correct distance so that $|C_{r_2}| = |C_r|$. Therefore, substituting Eq. (18) into (23) and simplifying, we get

$$T_r = \frac{\frac{bR_o}{R_q} T_r^n + T_r^{n'} - T_r^n}{\frac{bR_o}{R_q} T_r^n + 1 - T_r^n}. \quad (24)$$

Rearranging we get

$$T_r^n = \frac{\delta R_o}{R_q} \left[T_r^{n+1} - T_r^n \right] + T_r - \left[T_r^{n+1} - T_r^n \right] \quad (25)$$

or

$$n' = \frac{\ln \left\{ \frac{\delta R_o}{R_q} \left[T_r^{n+1} - T_r^n \right] + T_r - \left[T_r^{n+1} - T_r^n \right] \right\}}{\ln T_r} \quad (26)$$

Thus, once a value has been assumed for the threshold contrast or T_r of the black target against the horizon sky, Eq. (26) may be solved for various values of the background to equilibrium reflectance ratio $\delta R_o/R_q$ and n , the relative distance of the background from the threshold range r .

If $\delta R_o/R_q=0$, which is the case for a black background, Eq. (25) reduces to

$$T_r^n = T_r - T_r^{n+1} + T_r^n \quad (27)$$

This is equivalent to Eq. (6.32) of Middleton (1952). Middleton, however, does not extend the analysis to non-black backgrounds which Eq. (26) allows us to do.

Similarly if $\delta R_o/R_q=1$, which is the case for the horizon sky as background, Eq. (26) reduces to

$$n' = \frac{\ln T_r}{\ln T_r} = 1 \quad (28)$$

which means the target is at the threshold range r , as it should be.

Equation (26) has been evaluated for a threshold contrast of 0.05 in Table 5. The column for n' can be interpreted as the relative visual range since it is the distance related to the true visual range r , if the target is viewed against a non-horizon sky background. The column marked n is the background distance from the observer relative to the true visual range. The fourth column gives the background distance relative to the target distance. One of the constraints is the $n/n' \geq 1$ since this was one of the assumptions upon which the equation was developed.

Middleton (1952) suggested a background at least 1.5 times as far as the target, based on the black background equation evaluated for a threshold contrast of 0.02. The same rule-of-thumb is given by the WMO (1971) for the threshold contrast 0.025. A slightly larger relative distance is needed for the threshold contrast of 0.05 and a relative visual range of 0.935 with a black target and black background.

As can be seen, non-black backgrounds which have reflectances less than equilibrium, at the same relative distance beyond the target have relative visual ranges even closer to one than the black background. The non-black background simply approaches equilibrium radiance at

shorter distances. Thus the rule-of-thumb based on a black background works equally as well or rather better for non-black backgrounds equal to or less than the equilibrium reflectance.

For backgrounds brighter than equilibrium, such as a bright cloud, it is another matter. For these backgrounds it is necessary to have the background approximately twice as far as the target before the relative visual ranges are reasonably accurate.

The term $\delta R_o/R_q$ in Eq. (26) is similar to sky-ground ratio used historically in contrast transmittance computations. To avoid confusion, let us digress briefly to explain the meaning of the sky ground ratio.

Table 5.

Evaluation of Eq. (26) for a Threshold Contrast of 0.05 for Black Targets Viewed Against Backgrounds Other Than the Clear Horizon Sky

Background Relative Range n	$\delta R_o/R_q$	Relative Visual Range n'	Background/ Target Distance n/n'
1	0.0	.776	1.29
	0.5	.784	1.28
	0.8	.941	1.06
	1.0	1.000	1.00
	1.5	1.000	1.00
1.5	0.0	.935	1.60
	0.5	.965	1.55
	0.8	.985	1.52
	1.0	1.000	1.50
	1.5	1.036	1.45
	2.0	1.078	1.39
	4.0	1.333	1.13
	4.68	1.500	1.00
2.0	0.0	.983	2.03
	0.5	.991	2.02
	0.8	.995	2.01
	1.0	1.000	2.00
	1.5	1.007	1.99
	2.0	1.015	1.97
	5.0	1.069	1.87

Sky-Ground Ratio

When equilibrium luminance is constant with altitude the contrast transmittance equation can be written as [Duntley (1946), Eq. (36) p. 32 and Duntley (1948) Eq. (21)]

$$\frac{C_r(z, \theta, \phi)}{C_o(z_r, \theta, \phi)} = \left[1 + \frac{B_q(z, \beta)}{\delta R_o(z_r, \theta, \phi)} (T_r^{-1}(z, \theta) - 1) \right]^{-1} \quad (29)$$

where $B_q(\beta)$ is the equilibrium luminance for the path of sight. It is reasonably equivalent to the horizon sky luminance at an angle from sun β equal to the angle from sun of the path of sight θ, ϕ . It should be noted that the line of sight to the horizon used for the determination of the appropriate equilibrium luminance, will in general not be at the same azimuth as the path of sight used for determining the background luminance against which the target is viewed.

Equation (29) can be rewritten in terms of reflectance as follows

$$\frac{C_r(z, \theta, \phi)}{C_o(z_r, \theta, \phi)} = \left[1 + \frac{R_q(z, \beta)}{\delta R_o(z_r, \theta, \phi)} (T_r(z, \theta)^{-1} - 1) \right]^{-1} \quad (30)$$

Thus the sky-ground ratio is $B_g(\beta)/_b B_o$ or $R_g(\beta)/_b R_o$. It is a luminance ratio not an illuminance ratio like albedo. The sky ground ratio is the inverse of the ratio used in Eq. (26) and Table 5. Equation (30) refers to any target and any path of sight whereas Eq. (26) is limited to black targets and horizontal paths of sight.

Thus the sky-ground ratio was used with reference to contrast transmittance of an object against a non-sky background. It was a method of obtaining an indication of the degradation of contrast by the spacelight by using a horizon sky luminance at the correct angle from the sun β .

9. PHYSICAL MEASUREMENT METHODS

Direct physical measurement of air clarity appropriate to the human observer can be made by sensors filtered to produce a photopic response as specified by the C.I.E. Some of the most direct methods for specifying air clarity are to measure luminance transmittance, attenuation coefficient or total volume scattering coefficient. An alternate method of measuring the apparent radiance of distant dark targets and the horizon sky is also in current use. This review will not be exhaustive in terms of these techniques but each method will be described briefly as well as how they are relatable to the visibility range VV as specified by

$$VV = \frac{3}{\alpha} \quad (31)$$

which is consistent with Eq. (10).

Luminance Transmittance.

A transmissometer for measuring luminance transmittance utilizes a light source with known intensity I and a telephotometer at a known distance r . The relationship utilized is

$$E = \frac{I T_r(0, 90^\circ)}{r^2} \quad (32)$$

Thus by measuring the illuminance E , the transmittance T_r can be obtained.

The luminance transmittance is a function of the attenuation coefficient and the range r

$$T_r(0, 90^\circ) = e^{-\alpha(0)r} \quad (33)$$

This relationship can also be expressed as

$$\ln T_r(0, 90^\circ) = -\alpha(0)r \quad (34)$$

Now substituting in Eq. (31) we get

$$VV = \frac{3r}{-\ln T_r(0, 90^\circ)} \quad (35)$$

Middleton (1952) and more recently Douglas and Booker (1977) give detailed descriptions of transmissometers including calibration methods and error analyses. In addition, Douglas and Booker give a detailed history of the development and use of transmissometers for obtaining runway visual range.

Attenuation Coefficient.

The attenuation coefficient $\alpha(z)$ can be expressed as a function of the luminous path function $B_s(z, \theta, \phi)$ and the equilibrium luminance $B_g(z, \theta, \phi)$ (Eq. (11) of Duntley, *et al.* (1957))

$$\alpha(z) = \frac{B_s(z, \theta, \phi)}{B_g(z, \theta, \phi)} \quad (36)$$

All three parameters in Eq. (36) are point functions and may vary from point to point along a path of sight. If the atmosphere is reasonably homogeneous horizontally and the horizon is free of clouds, the horizon sky luminance is equal to the equilibrium luminance. The path function can be obtained by measuring the luminance of a black shadow box at a short path length from the photometer. The path function is in units of luminance per path length.

If the black box and the horizon sky luminance measurements are made by the same sensor, the absolute calibration is no longer important, only the precision of the two measurements, since any absolute error is factored out by using the ratio of the two values.

The visibility is obtained from the attenuation coefficient by means of Eq. (31). Instruments of this type were developed by Duntley shortly after the conclusion of the Tiffany experiments and are described most completely in Duntley, *et al.* (1957).

Total Volume Scattering Coefficient.

The total scattering coefficient $s(z)$ appropriate to the photopic sensor is equivalent to the attenuation coefficient in most cases since absorption is negligible in the visible spectrum for the fixed gases in the air and for clean fogs. Smoke and dust do absorb in the visible so that when these are present the total scattering coefficient will be less than the attenuation coefficient. Otherwise, the value of $s(z)$ is substituted for $\alpha(z)$ in Eq. (31) to obtain the visibility.

Beutell and Brewer (1949) described two basic types of total scattering meters which are in use currently. Both utilize the relationship

$$s(z) = \int_{4\pi} \sigma(z, \beta) d\Omega \quad (37)$$

where $\sigma(z, \beta)$ is the volume scattering function at angle β from the light source. Both schemes do the integration optically over nearly the complete 4π solid angle.

Both schemes measure $s(z)$ as a point function. If the horizontal layer of the atmosphere is not

homogeneous, this value is not applicable to the longer path indicated by the visibility distance. Some of this disadvantage can be overcome, however, by averaging over a period of time.

Diffuse Light Source. One scheme utilizes a diffuse or cosine light source to illuminate a volume of air. The sensor direction is perpendicular to the normal from the light source surface. Instruments of this type were used by Crosby and Koerber (1963) and more recently by Charleson, *et al.* (1967) and Horvath and Noll (1969) for environmental pollution studies.

Cosine Collector. The second scheme for measuring total volume scattering coefficient utilizes a diffuse or cosine collector on the sensor with a collimated light beam. It is the inverse of the first scheme. This second scheme has been utilized by Duntley, *et al.* (1970) and Duntley, *et al.* (1978) in studies of the optical properties of the troposphere, both daytime and nighttime.

Apparent Luminance of Distant Object and Sky.

Telephotometry of a distant mountain at known distance r and the horizon sky adjacent to it provides a measure of the apparent luminance of the target $B_r(0, 90^\circ, \phi)$ and the background $B_h(0, 90^\circ, \phi)$. This ratio is directly relatable to the apparent contrast by Eq. (1). If the inherent contrast is reasonably close to -1 and the path of sight is horizontal, the apparent contrast is also directly related to the attenuation coefficient $\alpha(0)$ by Eq. (8). Now combining Eqs. (1), (8), and (31), we get the visibility as a function of the distance to the target r and the ratio of the apparent radiance of the target and the horizon sky

$$V = \frac{3r}{-\ln \left| \frac{B_r(0, 90^\circ, \phi)}{B_h(0, 90^\circ, \phi)} - 1 \right|} \quad (38)$$

This method has the same advantage of being independent of absolute calibration errors as has the attenuation coefficient method if a single sensor is used to measure both the target and the horizon. It is, however, subject to the same errors as the visibility ranges obtained by observers if a non-black target is used. A measure of this error was depicted in Fig. 8. No attempt will be made herein to treat the problem of errors when a non-horizontal path of sight is used.

An indication of the inherent contrast can be obtained indirectly by a measurement of illuminance at the telephotometer site. This illuminance should be measured by a vertical illuminometer oriented so that the normal from the surface is 180 degrees from the path of sight azimuth, $E(0, 90, \phi+180^\circ)$. With this and the horizon sky luminance, the equilibrium reflectance can be computed from

$$R_q(0, 90^\circ, \phi) = \frac{B_r(0, 90^\circ, \phi) \pi}{E(0, 90^\circ, \phi+180^\circ)} \quad (39)$$

A ballpark estimate of the inherent reflectance of the target can probably be made, *i.e.* is the mountain forested,

rocky, snow capped, etc., and an estimate of C_v made accordingly. When R_q is fairly high, *i.e.* >1 , many natural surfaces will have inherent contrasts reasonably close to -1 as indicated by Fig. 9.

This method is subject to the same errors as the observed visibility when the background is other than the clear horizon sky (see Table 5).

This method was also investigated by Duntley when he developed the meter for measuring attenuation coefficient. He describes some of the theory and error analysis of a large base operation in Sect. V 5 of Duntley (1952). A slight modification of this method is discussed by Horvath and Presle (1978).

Telephotometry of distant objects using several narrow bands in the visible spectrum is described by Malm (1978). This method is currently being developed by EPA to use in monitoring the air quality in areas such as parks which are to be protected from pollution according to congressional mandate.

10. VISIBILITY BIBLIOGRAPHY

Recently a computerized search was conducted to obtain a bibliography on Visibility. This search was conceived as supplementing the annotated bibliography of Grimes (1969) which covers the period 1950-1969 and contains 179 references. Three library sources were searched as follows:

NTIS, 1969 to present, 185 references.

Physical Abstracts, 1969 to present, 193 references.

Meteorological and Geophysical Abstracts, 1970 to present, 209 references.

The beginning year for the search from the Meteorological and Geophysical Abstracts was simply the earliest available in computer form. All the listings included abstracts. It is expected that the listings from the three sources may be partially redundant, but the attempt was to obtain a fairly complete bibliography rather than a non-redundant one. Since each listing is in roughly chronological order, the composite bibliography is a viable source of further information.

No attempt has yet been made to review this bibliography or to include any portion herein due to its size. The total bibliography numbers 766 references.

11. SUMMARY

The daytime visibility is the distance an observer can see a black object against the horizon sky. The visibility as reported meteorologically correlates well with a contrast threshold of 0.05, and thus the visibility times the atmospheric attenuation coefficient is equal to 3. Psychophysical data on visual thresholds for 0.33 second glimpse times when corrected to confident viewing with a 4 degree uncertainty of target position, predict the visibility distances well and indicate that the observers are using targets subtending about 7.6 minutes of arc. Visibilities have an uncertainty of approximately ± 20 percent in relation to measured physical parameters of air clarity.

12. ACKNOWLEDGEMENTS

I would like to express appreciation to Richard W. Johnson for supporting and encouraging this review and gratitude to Seibert Q. Duntley for his critique. I also wish to thank Catharine F. Edgerton for contributing the pertinent meteorological background references and to thank Janet E. Shields for her detailed technical and editorial suggestions.

In addition, this report would not have been possible without the active support and contributions from the Visibility Laboratory, Editorial and Reproduction team: Mr. J. C. Brown, Ms. Alicia G. Hill, and Mr. James Rodriguez

13. REFERENCES

- Barteneva, O. D. (1960), "Scattering Functions of Light in the Atmospheric Boundary Layer," Bull. Acad. Sci. U.S.S.R., Geophysics Series, 1237-1244.
- Beutell, R. G. and A. W. Brewer (1949), "Instruments for Measurement of Visual Range," J. Sci. Instr. **26**, 357-359.
- Blackwell, H. R. (1946), "Contrast Thresholds of the Human Eye," J. Opt. Soc. Am. **36**, 624-643.
- Bricard, J. (1944), "La Visibilité des Objets éloignés à Travers le Brouillard," Ann. de Geophys. **1**, 101-112.
- Charlson, R. J., H. Horvath and R. F. Pueschal (1967), "The Direct Measurement of Atmospheric Light Scattering Coefficient for Studies of Visibility and Pollution," Atmospheric Environment **1**, 469-478.
- Crosby, P. and B. W. Koerber (1963), "Scattering of Light in the Lower Atmosphere", J. Opt. Soc. Am. **53**, 358-361.
- Douglas, C. A. and L. L. Young (1945), "Development of a Transmissometer for Determining Visual Range," U. S. Department of Commerce, Civil Aeronautics Administration, Washington, D.C., Technical Development Report No. 47.
- Douglas, C. A. and R. L. Booker (1977), "Visual Range: Concepts, Instrumental Determination and Aviation Applications," U. S. Department of Transportation, Federal Aviation Administration, Systems Research and Development Service, Report No. FAA-RD-77-8, Washington, D.C. 20590.
- Duntley, S. Q. (1946), *Visibility Studies and Some Applications in the Field of Camouflage*, Summary Technical Report, Dir. 16, NDRC, Columbia Univ. Press, New York, Vol. 2, Appendix A.
- Duntley, S. Q. (1948), "The Reduction of Apparent Contrast by the Atmosphere," J. Opt. Soc. Am. **38**, 179-191.
- Duntley, S. Q. (1952), "Visibility of Submerged Objects", Massachusetts Institute of Technology, Visibility Laboratory.
- Duntley, S. Q., A. R. Borleau, and R. W. Preisendorfer (1957), "Image Transmission by the Troposphere I," J. Opt. Soc. Am. **47**, 499-506.
- Duntley, S. Q., R. W. Johnson, and J. I. Gordon (1970), "Airborne Measurements of Optical Atmospheric Properties at Night," University of California, San Diego, Scripps Institution of Oceanography, Visibility Laboratory, SIO Ref. 70-7, AICRI-70-0137.
- Duntley, S. Q., R. W. Johnson, and J. I. Gordon (1972), "Airborne Measurements of Optical Atmospheric Properties in Southern Germany," University of California at San Diego, Scripps Institution of Oceanography, Visibility Laboratory, SIO Ref. 72-64, AICRI-72-0255.
- Duntley, S. Q., R. W. Johnson, and J. I. Gordon (1976), "Airborne Measurements of Optical Atmospheric Properties in Northern Germany," University of California, San Diego, Scripps Institution of Oceanography, Visibility Laboratory, SIO Ref. 76-17, AICRI-TR-76-0188.
- Duntley, S. Q., R. W. Johnson, and J. I. Gordon (1978), "Airborne Measurements of Optical Atmospheric Properties, Summary and Review III," University of California, San Diego, Scripps Institution of Oceanography, Visibility Laboratory, SIO Ref. 79-5, AICRI-TR-78-0286.
- Gordon, J. I. (1969), "Directional Radiance (Luminance) of the Sea Surface," University of California, San Diego, Scripps Institution of Oceanography, Visibility Laboratory, SIO Ref. 69-20.
- Grimes, A. (1969), "An Annotated Bibliography on Methods of Visibility Measurement, 1950-1969," Atmospheric Sciences Library ESSA ATS/IM LIB 2, Scientific Information and Documentation Division, Rockville, Md.
- Hering, W. S., H. S. Muench, and H. A. Brown (1971), "Field Test of a Forward Scatter Visibility Meter," Air Force Cambridge Research Laboratories, Hanscom Field, Bedford, Mass., AICRI-71-0315.
- Horvath, H. and K. E. Noll (1969), "The Relationship Between Atmospheric Light Scattering Coefficient and Visibility," Atmospheric Environment **3**, 543-550.
- Horvath, H. and G. Presle (1978), "Determination of Atmospheric Extinction Coefficient by Measurement of Distant Contrasts," App. Opt. **17**, 1303-1304.
- Houghton, H. G. (1939), "On the Relation Between Visibility and the Constitution of Clouds and Fog," J. Aer. Sci. **6**, 408-411.
- Koschmieder, H. (1924), "Theorie der Horizontalen Sichtweite," Beitr. Phys. freien Atm. **12**, 33-53; 171-181.
- Malm, W. C. (1978), "Multi-wavelength Contrast Telephotometry: Instrument Design and Data Interpretation", Proceedings Soc. Photo-Optical Inst. Eng. Vol. 42, 151-159.

Middleton, W.L.K. (1952), *Vision through the Atmosphere*, University of Toronto Press.

Moon, P. and D. F. Spencer (1942), "Illumination from a Non-Uniform Sky," *Illum. Eng.* 37, 707-726.

Shallenberger, G. D. and E. M. Little (1940), "Visibility through Haze and Smoke, and a Visibility Meter," *J. Opt. Soc. Am.* 30, 168-176.

Taylor, J. H. (1964), "The Use of Visual Performance Data in Visibility Prediction", *App. Opt.* 3, 562-569.

White, C. T. (1964), "Ocular Behavior in Visual Search", *Appl. Opt.* 3, 569-570.

World Meteorological Organization (1971), *Guide to Meteorological Instrument and Observing Practices*, Fourth Ed. Secretariat of the World Meteorological Organization, Geneva, Switzerland WMO-No. 8, TP. 3.

APPENDIX

OVERCAST SKY

One of the commonly used expressions to represent the overcast sky luminance is from Moon and Spencer (1942)

$$B(\theta) = B(90^\circ) [1 + 2 \cos \theta] \quad (A.1)$$

where θ is the zenith angle. The sky luminance is thus azimuth independent. Middleton (1952) Eq. (6.8) expresses this in the more general form

$$B(\theta) = B(90^\circ) [1 + m \cos \theta] \quad (A.2)$$

This relates the zenith and horizon luminances according to Table A.1.

Table A.1 Zenith to Horizon Relationships for the Modified Moon & Spencer Equation

m	Zenith Angle θ	
	0° Zenith	90° Horizon
0	1	1
1	2	1
2	3	1
3	4	1

The downwelling illuminance from Eq. A.2 is

$$E(0^\circ) = B(90^\circ) \int_0^{2\pi} \int_0^{\pi/2} (1 + m \cos \theta) \cos \theta \sin \theta d\theta d\phi \quad (A.3)$$

or

$$E(0^\circ) = B(90^\circ) \pi \left[1 + \frac{2m}{3} \right] \quad (A.4)$$

The modifier on the illuminance designates the zenith angle of the normal from the illuminometer. The average upwelling luminance \bar{B}_u is related to the albedo A by

$$\bar{B}_u = A \frac{E(0^\circ)}{\pi} = A B(90^\circ) \left[1 + \frac{2m}{3} \right] \quad (A.5)$$

The illuminance on a vertical plaque is the sum of the illuminance from half the sky $E(90^\circ, d)$ and from half the lower hemisphere or terrain $E(90^\circ, u)$

$$E(90^\circ) = E(90^\circ, d) + E(90^\circ, u) \quad (A.6)$$

The illuminance on the plaque from the terrain is

$$E(90^\circ, u) = \frac{\pi}{2} \bar{B}_u = A B(90^\circ) \pi \left[\frac{1}{2} + \frac{m}{3} \right] \quad (A.7)$$

The illuminance on the plaque from the sky is

$$E(90^\circ, d) = 2 \int_0^{2\pi} \int_0^{\pi/2} B(\theta) \cos \theta' \sin \theta d\theta d\phi \quad (A.8)$$

The angle θ' is the angle between the normal from the illuminometer at zenith angle 90° and the sky position at θ . Using the equation for rotation of coordinates to $\theta_1=90^\circ$ and $\phi_1=0$ from Gordon (1969) p. 45 Group A.12,

$$\cos \theta' = \sin \theta \cos \phi \sin \theta_1 \cos \phi_1 + \sin \theta \sin \phi \sin \theta_1 \sin \phi_1 + \cos \theta \cos \theta_1 \quad (A.9)$$

Since $\sin \theta_1 = \cos \phi_1 = 1$ and $\cos \theta_1 = \sin \phi_1 = 0$,

$$\cos \theta' = \sin \theta \cos \phi \quad (A.10)$$

Now substituting Eq. (A.2) and (A.10) into Eq. (A.8) we get

$$E(90^\circ, d) = 2B(90^\circ) \int_0^{2\pi} \int_0^{\pi/2} [1 + m \cos \theta] \sin^2 \theta d\theta \cos \phi d\phi \quad (A.11)$$

which when evaluated becomes

$$E(90^\circ, d) = B(90^\circ) \pi \left[\frac{1}{2} + \frac{2m}{3\pi} \right] \quad (A.12)$$

Thus the total illuminance on a horizontal plaque is the sum of Eq. (A.7) and (A.12)

$$E(90^\circ) = B(90^\circ) \pi \left[\frac{1}{2} (1 + A) + \frac{m}{3} \left(\frac{2}{\pi} + A \right) \right] \quad (\text{A.13})$$

The luminance of a vertical plaque of reflectance r_v would be

$$r_v B_v(90^\circ) = \frac{r_v E(90^\circ)}{\pi} \quad (\text{A.14})$$

$$= r_v B(90^\circ) \left[\frac{1}{2} (1 + A) + \frac{m}{3} \left(\frac{2}{\pi} + A \right) \right]$$

This is equivalent to Eq. (6.14) in Middleton (1952)

A useful term in evaluating contrasts against the horizon sky background is the equivalent reflectance of the horizon sky,

$$r_h R(90^\circ) = \frac{B(90^\circ) \pi}{E(90^\circ)} \quad (\text{A.15})$$

Substituting in Eq. (A.13) for $E(90^\circ)$ we get

$$r_h R(90^\circ) = \left[\frac{1}{2} (1 + A) + \frac{m}{3} \left(\frac{2}{\pi} + A \right) \right]^{-1} \quad (\text{A.16})$$

DATE
FILMED
-8